A&A 409, 205–215 (2003)
DOI: 10.1051/0004-6361:20031070

Astronomy & Astrophysics

Research Note

A three-dimensional Galactic extinction model

R. Drimmel[1], A. Cabrera-Lavers[2], and M. López-Corredoira[3]

[1] Istituto Nazionale di Astrofisica (INAF), Osservatorio Astronomico di Torino, 10025 Pino Torinese, Italy
[2] Instituto de Astrofisica de Canarias, 38200 La Laguna, Tenerife, Spain
[3] Astronomisches Institut der Universität Basel, Venusstrasse 7, 4102 Binningen, Switzerland

Received 2 May 2003 / Accepted 2 July 2003

Abstract. A large-scale three-dimensional model of Galactic extinction is presented based on the Galactic dust distribution model of Drimmel & Spergel (2001). The extinction A_V to any point within the Galactic disk can be quickly deduced using a set of three-dimensional Cartesian grids. Extinctions from the model are compared to empirical extinction measures, including lines-of-sight in and near the Galactic plane using optical and NIR extinction measures; in particular we show how extinction can be derived from NIR color-magnitude diagrams in the Galactic plane to a distance of 8 kiloparsec.

Key words. dust, extinction – ISM: structure – Galaxy: structure

1. Introduction

In the past a fundamental obstacle to Galactic studies has been extinction due to interstellar dust, which has limited our view of the Galactic stellar distribution to the solar neighborhood. During the past decade NIR surveys, together with ever deeper optical surveys, have been piercing the interstellar haze, probing the stellar distribution in the Galactic plane and revealing its nonaxisymmetric structure, including the barred nature of the Galactic bulge (Blitz & Spergel 1991; Weiland et al. 1994), the Galactic warp (Djorgovski & Sosin 1989; Freudenreich et al. 1994) and the spiral arms (Drimmel 2000; Bissantz & Gerhard 2002). Newly available high-resolution NIR surveys, such as 2MASS and DENIS, promise to further reveal the nature of these structures. However, while the effects of interstellar dust are mitigated at NIR wavelengths, they are still important.

The most recent map of Galactic extinction over the entire sky is that of Schlegel et al. (1998, hereafter SFD), however it only maps the *total* Galactic extinction and is therefore most appropriate for extragalactic studies. To study stellar populations or objects found throughout the Galactic disk a volumetric description of Galactic extinction is required. Three-dimensional extinction models have been produced using reddening data from stellar samples (Neckel et al. 1980; Arenou et al. 1992; Hakkila et al. 1997; Mendez & van Altena 1998), but these give only a local description of extinction, being reliable to heliocentric distances of about 2 kiloparsecs due to limited sampling at optical wavelengths. However, in the NIR a well-defined stellar population can provide extinction measures along a line-of-sight to much greater distances; here we describe in detail one such method, deriving extinction measures from NIR color-magnitude diagrams (CMDs) using the known properties of the red-clump giants. This method is capable of rendering extinctions to distances as far as 8 kpc in the Galactic plane.

In lieu of empirical extinction measures, a three-dimensional Galactic dust distribution model can be adopted from which extinction is derived. Previous studies at high and mid galactic latitudes have used "slab" models, where a vertical dust density profile is adopted. Chen et al. (1999) have extended the usefulness and accuracy of such a model to relatively low latitudes by renormalizing their model to the SFD extinction map. Large-scale models that describe the dust distribution over the entire Galactic disk have in the past been axisymmetric, correlating the radial variation of the dust distribution with that of the gas (hydrogen) surface density, derived from HI, HII and CO observations together with assumed values and gradients for the gas:dust (metallicity) and CO:H_2 ratios (e.g. Wainscoat et al. 1992; Ortiz & Lepine 1993). Recently models have been constructed based upon FIR data, where Galactic emission is dominated by the thermally radiating dust. Initially these models were also axisymmetric (Spergel et al. 1996; Davies et al. 1997), but more recently have adopted nonaxisymmetric structures to account for their observed FIR emission, including the Galactic warp and spiral arms (Drimmel & Spergel 2001; Launhardt et al. 2002).

Here we present for general use a large-scale three-dimensional model of Galactic extinction based on the Galactic

Send offprint requests to: R. Drimmel,
e-mail: drimmel@to.astro.it

dust distribution model of Drimmel & Spergel (2001, hereafter DS01). The following two sections describe the construction and application of the extinction model. In section four we describe how empirical extinction measures can be derived from NIR CMDs, and we compare the predictions of the model with these and other extinction measures. The summary section details a number of caveats that a potential user of the model should be aware of.

2. Galactic extinction model

Given a three-dimensional model of the dust distribution, $\rho_{\rm d}(\boldsymbol{x})$ the extinction in a given direction can be found by integrating along a line-of-sight to the point of interest,

$$A_V(\boldsymbol{x}) = 1.086\tau_{\rm V} = 1.086\kappa_{\rm V}\int_0^{\boldsymbol{x}} \rho_{\rm d}\,{\rm d}s, \tag{1}$$

while the total Galactic extinction is found by integrating to infinity. The model of the dust distribution is detailed in DS01. We mention here that this model is composed of three structural components: a warped, but otherwise axisymmetric disk with a radial temperature gradient, spiral arms as mapped by known HII regions, and a local Orion-Cygnus arm segment. The structural parameters of the dust model are constrained by the FIR observations of the COBE/DIRBE instrument, while the determination of the parameter $\kappa_{\rm V}$, and the decomposition of the flux density into dust density and emissivity, is achieved by modeling the extinction in the COBE/DIRBE NIR observations. However, the model as presented here has been amended in its description of the spiral arm geometry.

The previous spiral arm geometry used in DS01 was based on the mapping of Galactic HII regions (Georgelin & Georgelin 1976; Taylor & Cordes 1993). Due to a lack of data, this map did not extend to the opposite side of the Galaxy. In order to provide a realistic model of the spiral arm contribution over the whole of the Galaxy, the extended geometry of Bland-Hawthorn & Maloney (2002) is adopted. Figure 1 shows the dust surface density of the model, including the new spiral arm component. No other parameters of the dust model have been changed, and in fact the extension of the arms does not lead to any significant differences in the FIR emission profiles as predicted by the model of DS01, because the spiral arms on the far-side of the Galaxy are unresolved in the FIR DIRBE data. This model will need further refinement once FIR emission toward the Galactic center is considered, as it predicts arm tangents within $|l| < 20^\circ$ which are not evident in the Galactic plane FIR emission profile.

Another feature of the dust model of DS01 is the use of direction-dependent rescaling factors that are based on the FIR residuals between the DIRBE 240 μm data and the predicted emission of the parametric dust distribution model, and that effectively "correct" the dust column density of the smooth model to account for small (angular) scale structure not described explicitly by the model. In practice, for any given DIRBE pixel, one of the three structural components is rescaled to reproduce the FIR flux. The component chosen for rescaling is typically that which needs the least fractional change in its column density to account for the FIR residual, though the spiral arms are preferentially chosen near the Galactic plane (see DS01 for details). The effect of the rescaling factors is to add (detract) dust along the entire line-of-sight *for the rescaled component only*, therefore their application represents an approximate correction to the model in the sense that no bias with respect to distance is effected, apart from that described by the rescaled component. It should also be noted that the rescaling procedure implicitly assumes that the deviation between the predicted and observed FIR emission is *not* due to variations in dust temperature.

Fig. 1. Map of the dust surface density from the dust distribution model with the extended geometry for the spiral arms. The Sun's location is indicated by the point at center-left.

In DS01 the rescaling factors were used to refine the dust model when accounting for extinction in their modeling of the J and K band emission observed by COBE, hence only applied for galactic latitudes $|b| < 30^\circ$. As a practical matter, the rescaling factors for latitudes $|b| > 30^\circ$ are based on the SFD Galactic extinction map, as the low signal-to-noise of the 240 μm emission at high galactic latitudes does not allow their reliable determination. Rescaling to the SFD extinction map was done as follows: The rescaled dust density can be expressed as

$$\tilde{\rho}_{\rm d} = \sum f_i \rho_i \tag{2}$$

where the sum is over the structural components of the dust density model (i = disk, spiral arms, local Orion arm), and the rescaling factors f_i are direction dependent, i.e. $f_i(l, b)$. Rescaling is applied to only one component, so that at most one of the factors $f_i \neq 1$ for a given line-of-sight. For any given direction the total extinction is then

$$\tilde{A}_V(\infty) = \sum f_i A_i(\infty), \tag{3}$$

where

$$A_i(\infty) = 1.086\kappa_{\rm V}\int_0^{\infty} \rho_i\,{\rm d}s, \tag{4}$$

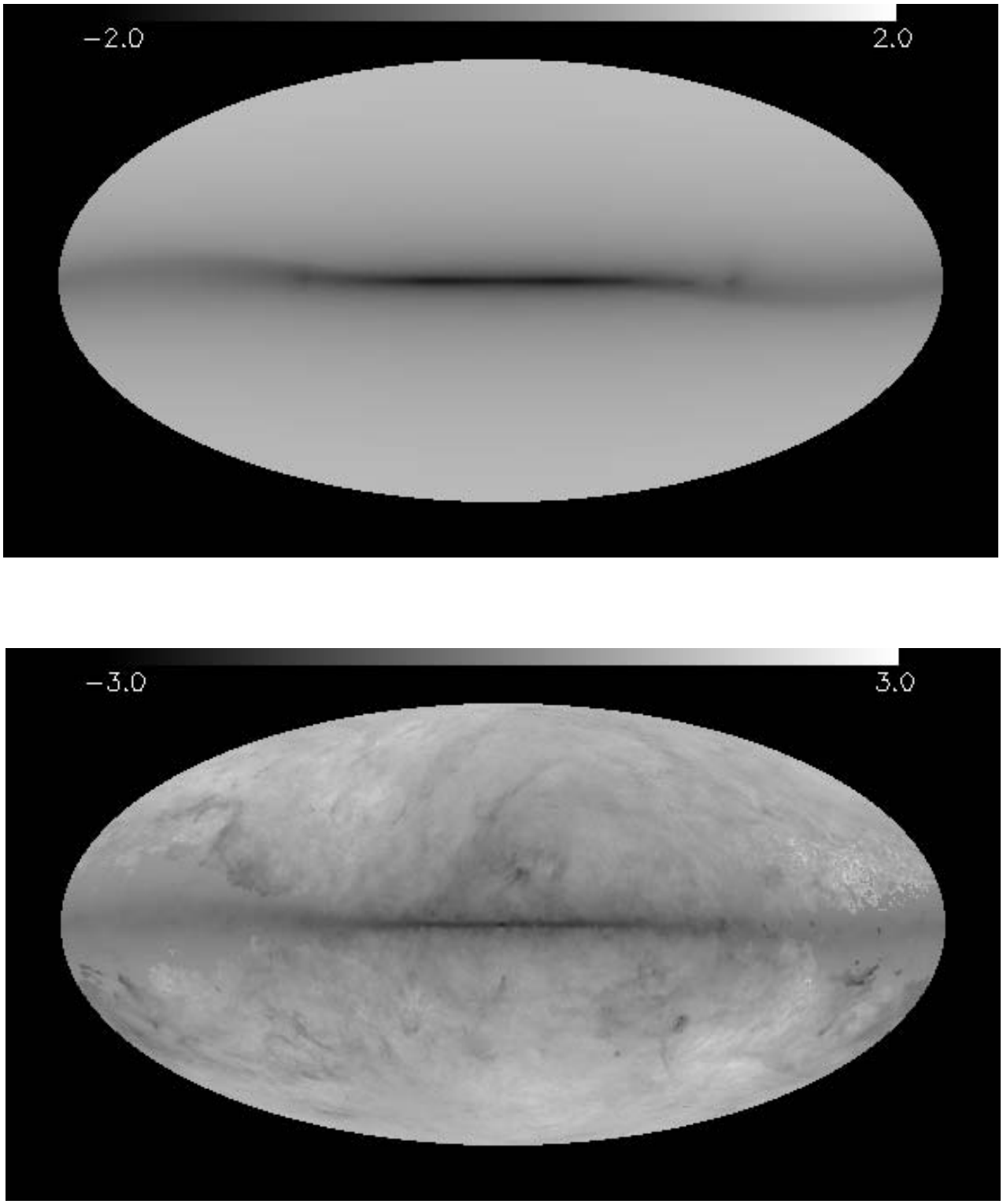

Fig. 2. Sky maps of the predicted total Galactic extinction in a Mollweide projection, without (top) and with (bottom) rescaling. The direction to the Galactic center is at the center of the plot, positive galactic longitudes to the left. The quantity plotted in grey scale is $-\log(A_V)$.

the integral being taken along the line-of-sight, ρ_i corresponding to the dust density associated with component i and κ_V is the mean opacity. Rescaling to the SFD extinction map, $A_{\rm SFD}$, is effected by insisting that $\tilde{A}(\infty) = A_{\rm SFD}$, which leads to

$$f_{\rm disk} = \frac{A_{\rm SFD} - \sum_{i\neq{\rm disk}} A_i(\infty)}{A_{\rm disk}(\infty)}. \quad (5)$$

Only the disk component need be rescaled, as at high Galactic latitudes it is only this component that contributes significantly to the dust column density.

Figure 2 shows the skymaps of total Galactic extinction, both with and without rescaling. Rescaling effectively adds angular detail that is not described by the parametric dust model.

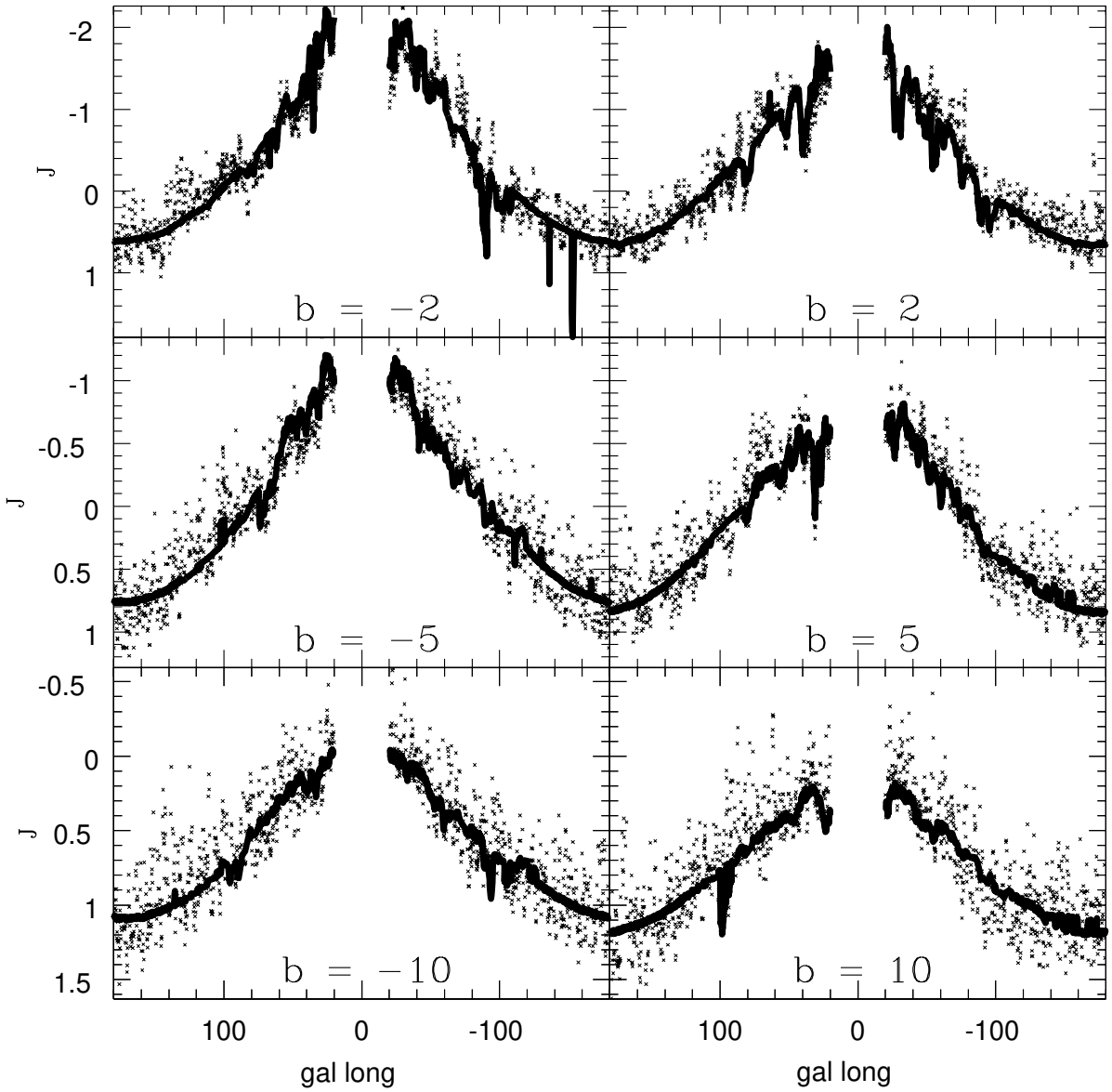

Fig. 3. *J* band emission profiles at low galactic latitudes, as observed by the COBE satellite (crosses) and predicted by the dust model using rescaling factors (from DS01).

To give the reader an appreciation of the importance of the rescaling factors at low galactic latitudes, *J* band emission profiles are shown in Figs. 3 and 4 that both employ and neglect their use.

3. Application

An estimate of the extinction to any point within the Galaxy using the rescaling factors can be achieved by either integrating the rescaled dust model, $\tilde{\rho}_{\rm d}$, along the line-of-sight to the point of interest (Eq. (1) with $\tilde{\rho}_{\rm d}$),or by summing over the extinction contributions of each component, determined separately via a line-of-sight integration, and applying the rescaling factor to the appropriate component. However, such integrations are time consuming, especially if many lines-of-sight need to be considered. To provide a more efficient means of finding the extinction within the Galactic disk we have constructed a set of three-dimensional Cartesian grids of extinction in V, each corresponding to a separate component of the dust model, as well as a table of the rescaling factors described above. Both large-scale and small scale grids are provided; the former cover the entire Galactic disk while the later describe the extinction about the Sun in greater detail. Using the three-dimensional extinction grids a value for the extinction A_i due to each of the components i of the dust distribution can be found for any point in the Galactic disk via interpolation. Together with the appropriate rescaling factor a final estimate of the extinction is arrived at:

$$\tilde{A}_V(l,b,r) = \sum f_i(l,b) A_i(l,b,r). \tag{6}$$

Trilinear interpolation from the grids described above is orders of magnitude faster than numerically integrating the dust model to individual sources, and the interpolation error is of the order of 0.2%.

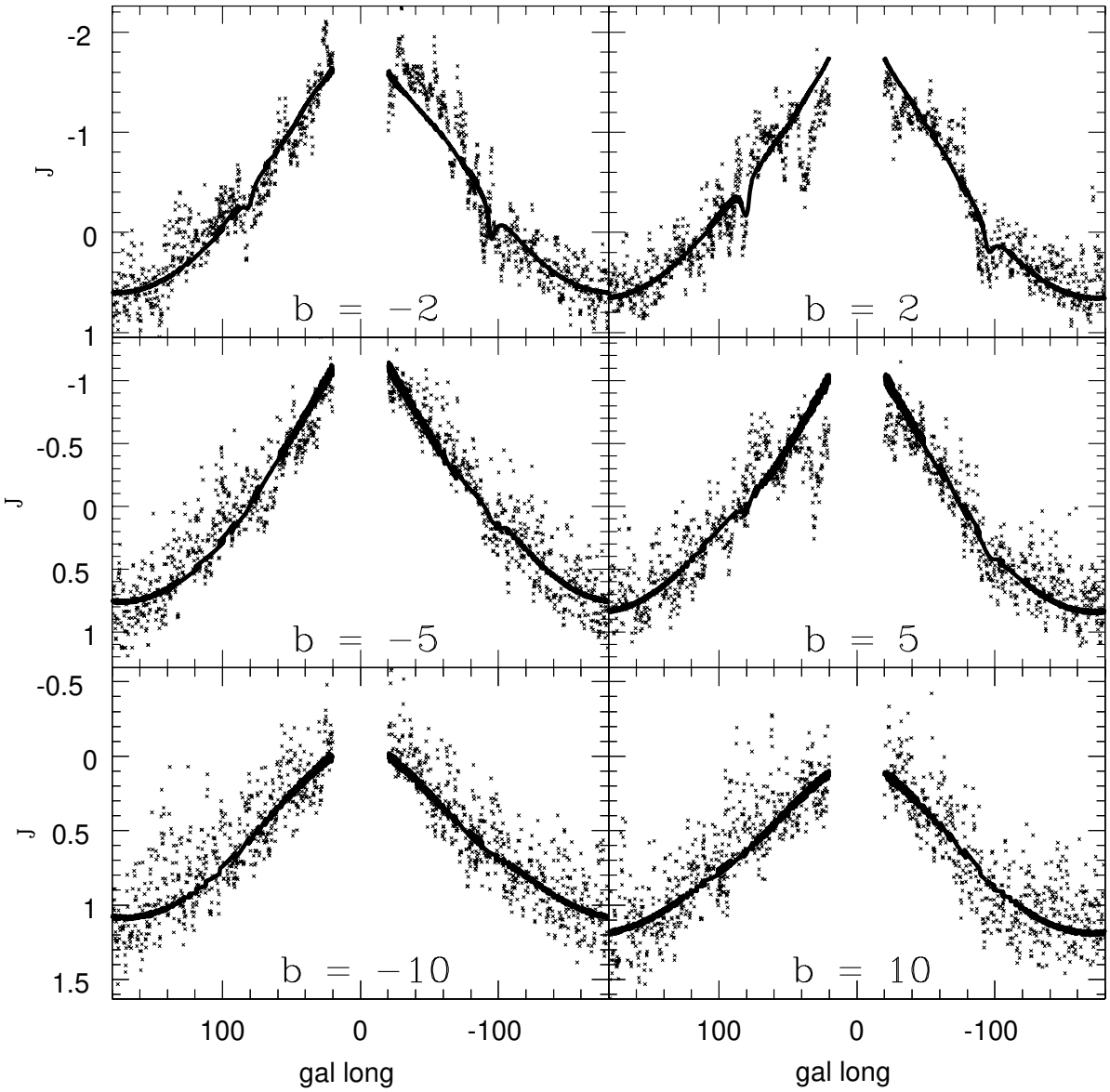

Fig. 4. As in previous figure, but using the dust model without rescaling factors.

As an example, Fig. 5 shows a slice in the Galactic plane through the large-scale grid for the spiral arm component. Both this grid and that of the disk component have *xyz* dimensions of $30 \times 30 \times 1$ kpc, the $z = 0$ plane corresponding to the Galactic plane. Thus they describe the extinction out to a galactocentric radius of $R = 15$ kpc. The grid spacing parallel to the Galactic plane is 200 pc, while perpendicular to the plane the resolution is 20 pc. Meanwhile, the large-scale grid for the Orion arm component has reduced dimensions and finer grid spacing parallel to the Galactic plane, so that it covers only part of the Galaxy, having dimensions of $3.75 \times 7.5 \times 1$ kpc.

To provide greater detail near the Sun and to avoid interpolation errors, two local grids are constructed, one for the Orion arm and another for the disk component; the spiral arm component does not make a significant contribution near the Sun. Both grids have their *xy* coordinates centered on the Sun, though with different grid spacing in the *xy* directions. (The grid spacing in the z direction for all grids is $\Delta z = 0.02$ kpc.) The second of these local grids, that of the disk component, is necessary only to avoid interpolation errors which would otherwise be greater than 5% for heliocentric distances less than 500 pc with the larger grid spacing of the large-scale grid. Ideally this region about the Sun should be described by a more detailed local model of the dust distribution.

The rescaling factors over the entire sky are also supplied on the same resolution as the FIR COBE/DIRBE data: Because the rescaling factors are based on the residuals between the DIRBE FIR observations and the predictions of the dust distribution model, the rescaling factors are rooted to the DIRBE data structure; for each DIRBE pixel there is an associated rescaling factor. This introduces some complication in the retrieval of the rescaling factors for arbitrary directions as the DIRBE sky maps use a non-standard projection and a binary pixel ordering scheme. (See `http://lambda.gsfc.nasa.gov/product/cobe/skymap_info.cfm` for a brief introduction and

Fig. 5. Extinction in the Galactic plane due to the spiral component of the dust distribution out to $R = 15$ kpc from the Galactic center. The Galactic center is at center, with the Sun located at center-left. The tangents to the spiral arms are clearly evident. The maximum extinction is 5.7 mag in V.

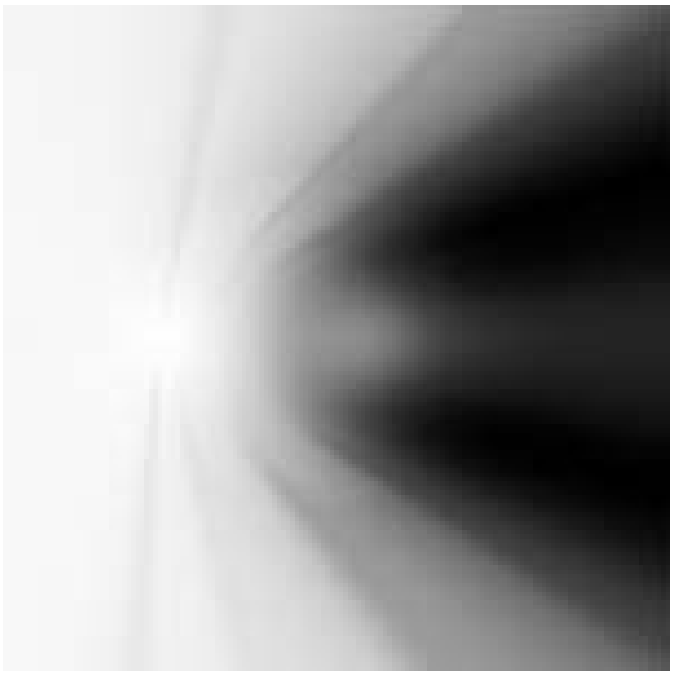

Fig. 6. Extinction map in the Galactic plane resulting from all components of the dust model (disk, spiral arms and the local Orion-Cygnus arm). Orientation and scale is as in the previous diagram and the maximum extinction is 37 mag in V.

Appendix G of the COBE Guest Investigator Software (CGIS) Software User's Guide (version 2.2), retrievable at `http://lambda.gsfc.nasa.gov/product/cobe/cgis_docs.cfm`, for further details.) To apply the rescaling factors the user must determine the DIRBE pixel that corresponds to the direction of interest. There are at least three options for this:

1. Write a routine that searches through the entire list of pixel coordinates for the nearest pixel.
2. Work within the IDL environment developed by the COBE data reduction team which provides an efficient means, via CGIS IDL code, to retrieve the pixel number nearest a given direction. This IDL package with instructions for installation can be found at `http://lambda.gsfc.nasa.gov/product/cobe/cgis.cfm`.
3. Use stand alone CGIS standard FORTRAN code to retrieve the pixel number for a given direction. This code can also be found at the above URL.

Thus a file is provided for the user containing, for each DIRBE pixel, the DIRBE pixel number, its galactic coordinates, an index of the component to be rescaled and its rescaling factor. This file, together with those containing the extinction grids and detailed instructions for their use, can be found at the anonymous ftp site `ftp://ftp.to.astro.it/astrometria/extinction/`.

To summarize, an algorithm for finding the extinction A_V to a point in the Galaxy (l, b, r) is outlined below:

- Find the COBE pixel coinciding to (l, b).
- Recover the rescaling factor f_i and component i to be rescaled. (Set $f = 1$ for the other components.)
- Determine the grid coordinates: $(l, b, r) \longrightarrow (x, y, z) \longrightarrow (i, j, k)$
- Interpolate from appropriate grids to find $A_i(l, b, r)$ for each component.
- Sum over the components (Eq. (6)) to arrive at $\tilde{A}_V(l, b, r)$.

An example of IDL and FORTRAN code that performs the above algorithm can be found on the anonymous ftp site mentioned above.

It is important to note that if one decides *not* to use the rescaling factors it is sufficient to use only two grids, a large-scale and a local grid, which are each a sum of the grids mentioned above, and perform only a single interpolation from the appropriate grid. Figure 6 shows the resulting large scale grid, also provided to the user. One might wonder why the same is not done above, that is, construct a single three-dimensional grid of the final rescaled $\tilde{A}_V(i, j, k)$. The reason is that the use of the rescaling factors would introduce discontinuities in such a grid, rendering interpolation unreliable; first interpolation must be done on each (smooth) component, then the direction dependent rescaling factor applied.

As a final detail we mention that the extinction from the model, given in the V band, can be transformed to other wavebands using the (A/A_V) ratios given by Rieke & Lebofsky (1985). Recently there has been some debate whether these ratios may be too high in the NIR (Glass 1999; Draine 2003), however these ratios are preferred here in order to remain consistent with the NIR modeling of DS01. It should also be noted that if using these ratios one assumes a specific reddening curve

which in practice is spatially variable blueward of the Johnson *R* band (Mathis 1990; Fitzpatrick 1999).

4. Comparing model with data

The Galactic extinction map of SFD , $A_{\rm SFD}$, and of the extinction model, A_∞, are both based in part on COBE FIR data, however the maps were derived using different approaches. It is therefore interesting to compare the two extinction maps *before* using the SFD map to rescale the high latitude data. The two maps of Galactic extinction were compared for each COBE pixel between galactic latitudes $5^\circ < |b| < 40^\circ$. The lower boundary is the limit of reliability for $A_{\rm SFD}$ as stated by Schlegel et al. (1998), while above $|b| = 40^\circ$ the 240 μm data becomes too noisy to derive reliable rescaling factors. In addition data in the directions of the Orion nebula, Rho Ophiucus, Andromeda and the LMC and SMC were removed. The mean residual of the remaining data, $\langle A_{\rm SFD} - A_\infty \rangle$, was found to be 0.096 mag, while the mean relative difference, $\langle (A_{\rm SFD} - A_\infty)/A_{\rm SFD} \rangle$, was equal to 0.024, showing that the two maps have nearly the same normalization. This concordance between the two extinction maps is the reason why the boundary for the different rescaling schemes at $|b| = 30^\circ$ is hardly evident in Fig. 2. However, the mean *absolute* residual, $\langle |A_{\rm SFD} - A_\infty| \rangle$ has a value of 0.15 mag, and a mean relative absolute difference of 0.19, showing that there is substantial scatter in the difference between the two maps.

However, rather than provide a sky map of the total Galactic extinction, the primary purpose of the extinction model is to give an estimate of extinction to any point *within* the Galactic disk. To evaluate the model's performance in this regime we compare extinction estimates from the model with empirical extinction measures using NIR data from the second incremental data release (2IDR) of the 2MASS[1] project (Skrutskie et al. 1997, 2000, `http://www.ipac.caltech.edu/2mass/releases/docs.html`).

In López-Corredoira et al. (2002, hereafter L02) a method was presented to obtain both the star density and interstellar extinction along a line-of-sight by extracting the well-known red-clump population (spectral type K2III) from the infrared color-magnitude diagram (CMD). These stars constitute the majority of the disc giants (Cohen et al. 2000; Hammersley et al. 2000) and can be easily identified in the NIR CMDs. The method is extensively described in L02, so we give only a brief summary with some additional details here.

$(J-K, m_K)$ CMDs are built for $1^\circ \times 1^\circ$ fields by using available 2MASS data. In these diagrams stars of the same spectral type (i.e. the same absolute magnitude) will be placed at different locations in the CMD; the effect of distance and extinction cause the red-clump giants to form a broad diagonal branch running from top left to bottom right in the CMDs. In order to isolate the red-clump sources in the CMD we use theoretical traces of different spectral types, based on the updated "SKY" model (Wainscoat et al. 1992), to define the possible color range of the K-giant branch in the CMDs, without any further implication in the method. (The "SKY" model uses a double exponential disk for the dust distribution, used here to roughly approximate interstellar extinction.) For each field appropriate traces are chosen to isolate the K-giants and avoid contamination by other stellar populations, especially dwarf stars and M-giants (see Fig. 7).

[1] 2MASS is a joint project of the Univ. of Massachusetts and the Infrared Processing and Analysis Center, funded by NASA and NSF.

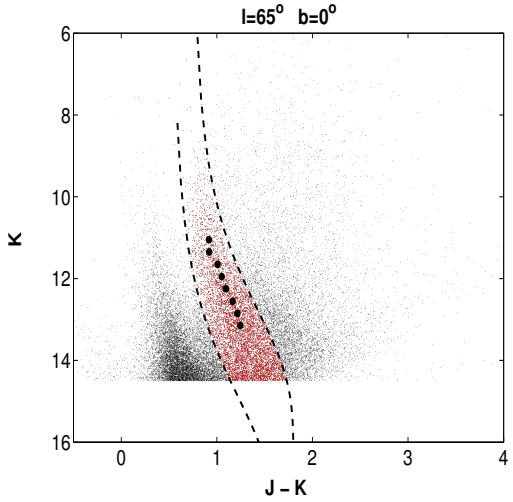

Fig. 7. NIR color-magnitude diagram for a typical low-latitude field ($l = 65^\circ$, $b = 0^\circ$), taken from the 2MASS survey. Dashed curves delineate the selected region isolating the red-clump giants. Filled circles show the maxima of the red-clump for individual magnitude bins.

Once the optimal traces have been selected, the giant stars are extracted from the CMD and binned in apparent K magnitude, m_K. For each magnitude bin, count histograms in color are constructed. A Gaussian function was then fit to the histograms to determine the color of the peak counts at each magnitude:

$$f(x; A, \mu, \sigma) = A \exp[-(x-\mu)^2/2\sigma^2], \tag{7}$$

where x is the binned $(J-K)$ color and μ is taken as the color of the peak. Figure 8 shows the Gaussian fits to the color histograms obtained at three different magnitude bins for the field of Fig. 7. The maxima are identified as corresponding to the mean observed color $(J-K)_{m_K}$ of the K2III stars at the given apparent magnitude m_K since they are by far the most prominent population in the selected region. (See also Fig. 2 in L02 for further details).

The extinction $A_K(m_K)$ can be determined by tracing how the peak $(J-K)$ of the red-clump counts changes with m_K and adopting an intrinsic mean color $(J-K)_0$ of the red-clump. From the color excess and after Rieke & Lebofsky (1985):

$$A_K(m_K) = \frac{(J-K)_{m_K} - (J-K)_0}{1.52}. \tag{8}$$

Once the extinction A_K is estimated at the apparent magnitude m_K, a mean distance to the stars can then be found given their mean absolute magnitude. For the K2III population the mean absolute magnitude and the intrinsic color were assumed to be $M_K = -1.65$ and $(J-K)_0 = 0.75$, with a Gaussian dispersion of 0.3 mag in absolute magnitude and 0.2 in color (see L02). Recent results in open clusters yield very similar values: Grocholski & Sarajedini (2002) obtained $M_K = -1.62$ with a standard deviation of 0.21 and mean color $(J-K)_0$ of around

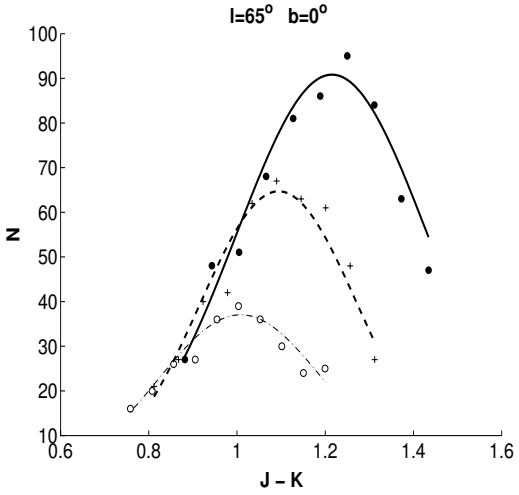

Fig. 8. Gaussian fits (lines) to the red-clump counts (points) in three magnitude bins for the field $l = 65°$ $b = 0°$. Solid line (filled circles) corresponds to the $12.7 < m_K < 13$ bin, the dashed line (pluses) to the $12.1 < m_K < 12.4$ bin, and the dot–dashed line (open circles) to the $11.5 < m_K < 11.8$ bin

0.7 for the old disc population, with small dispersion due to metallicity or age gradients, while Pietrzyński et al. (2003) show that the K-band magnitude of the red-clump is a good distance indicator, independent of the metallicity and age, with some small dispersion in the color dependence.

Uncertainties of the extinction were estimated from the uncertainty of the mean color of the Gaussian component:

$$\sigma_{A_K} = \sigma/(1.52\sqrt{N}) \tag{9}$$

where σ is the standard deviation of the fitted Gaussian and $N = A\sigma\sqrt{2\pi}$ is the estimated number of red-clump stars. This uncertainty gives an indication of the statistical error only, and does not include other possible systematic errors. Some uncertainties of the method, such as metallicity effects for the clump giants or differences between the real red-clump color distribution and the assumed Gaussian function are fully described in L02, so they will not be repeated here.

Critical aspects that are to be considered in the Gaussian fit are the possible contamination by dwarf stars and the effect of the completeness limit of the 2MASS survey. For fields such as those used here, dwarf contamination is negligible for $m_K \approx 13$ (see Sect. 3.3 in L02 for details) while the 2MASS survey is complete up to magnitudes of $m_K \approx 14$. For this reason, the Gaussian fits have been obtained in each field only up to $m_K \approx 13$, well above the completeness limit of the survey and where the dwarf contamination is small.

This method has been used for near-plane regions in both the outer and inner Galactic disc (L02; Lopez-Corredoira et al. 2003, in preparation) with very satisfactory results. Some estimations of interstellar extinction have also been obtained in this way for the star count predictions of the *Besançon model* (Robin & Creze 1986) in the Galactic Plane and the results shown there are in good agreement between the observed extinction in the K-band and the model predictions (Picaud et al. 2003). The main strength of the method is that it is empirical and we can extract the red-clump giants from the CMDs assuming only their mean absolute magnitude and intrinsic color.

Figures 9 and 10 show the extinction along selected lines-of-sight in and near the Galactic plane as given by the extinction model and the NIR data. Also shown where available are extinction measures from individual OB stars from the Neckel et al. compilation (Neckel et al. 1980, 1995). These extinctions are converted to the K band using $(A_K/A_V) = 0.112$ as given by Rieke & Lebofsky (1985). When present these give a measure of the extinction out to a couple of kiloparsecs from the Sun, whereas the NIR red-clump data give a measure of extinction as far as 8 kpc. In general the NIR extinction measures are more reliable as each measure (distance and extinction) is based on many stars, as described above. In addition the distances of the OB stars are spectro-photometric, and thus suffer from large uncertainties due to misclassification and cosmic variation.

In Fig. 9 lines-of-sight with and without OB stars are presented; in those fields containing no OB stars (left column) there is good agreement between the model and the NIR extinction measures, while in those fields containing many OB stars the model is consistently giving higher extinction than indicated by the NIR data. This can partly be understood by the effect of the OB stars on their environment, as they will heat the ambient dust leading to higher dust emission than is typically seen in the arms. This contributes to the erroneous rescaling seen in the field at $l = 173°$. Also worth noting for this field, as well as that at $l = 187°$, is that the two data sets give inconsistent measures of the extinction, which must monotonically increase with distance. This inconsistency might in part be accounted for if the extinction curve for these lines-of-sight were nonstandard, i.e. $R_V = 5$ rather than the canonical value of 3.1. In this case the extinctions of the OB stars would systematically decrease by approximately 3/5ths while their distances would increase, giving much better agreement with the NIR data which is insensitive to variations in the extinction curve. In any case, the model falls between the two empirical measures for these two fields.

For the inner disk (Fig. 10) the deviations between the data and the model are not as easily understood. Typically these deviations are of the order of 20%, though seem to be higher in directions corresponding to tangents of spiral arms ($l = 50°$ and 30°). Also shown for some of these lines-of-sight is the extinction curve for a model in which the disk was rescaled rather than the nominally selected spiral arms. The performance of this alternative rescaling is in general not significantly worse nor better, though it seems to be better along spiral arm tangents and worse in other directions. The exception is in the direction $l = 50°$, which is much better. However, this apparent improvement may be misleading, as the failure of the model may lie in its assumed geometry of the Sag-Car spiral arm, which places its tangent inside of $l = 50°$. The direction $l = 75°$ is influenced by the local Orion-Cygnus arm, but shows good agreement with the NIR data out to a distance of 4 kpc, at which point the NIR data shows a large step in extinction. (The non-scaled extinctions suffer artifacts from interpolation errors as the single grid containing the dust model does not have sufficiently small gridding to resolve this feature.) Again, for this

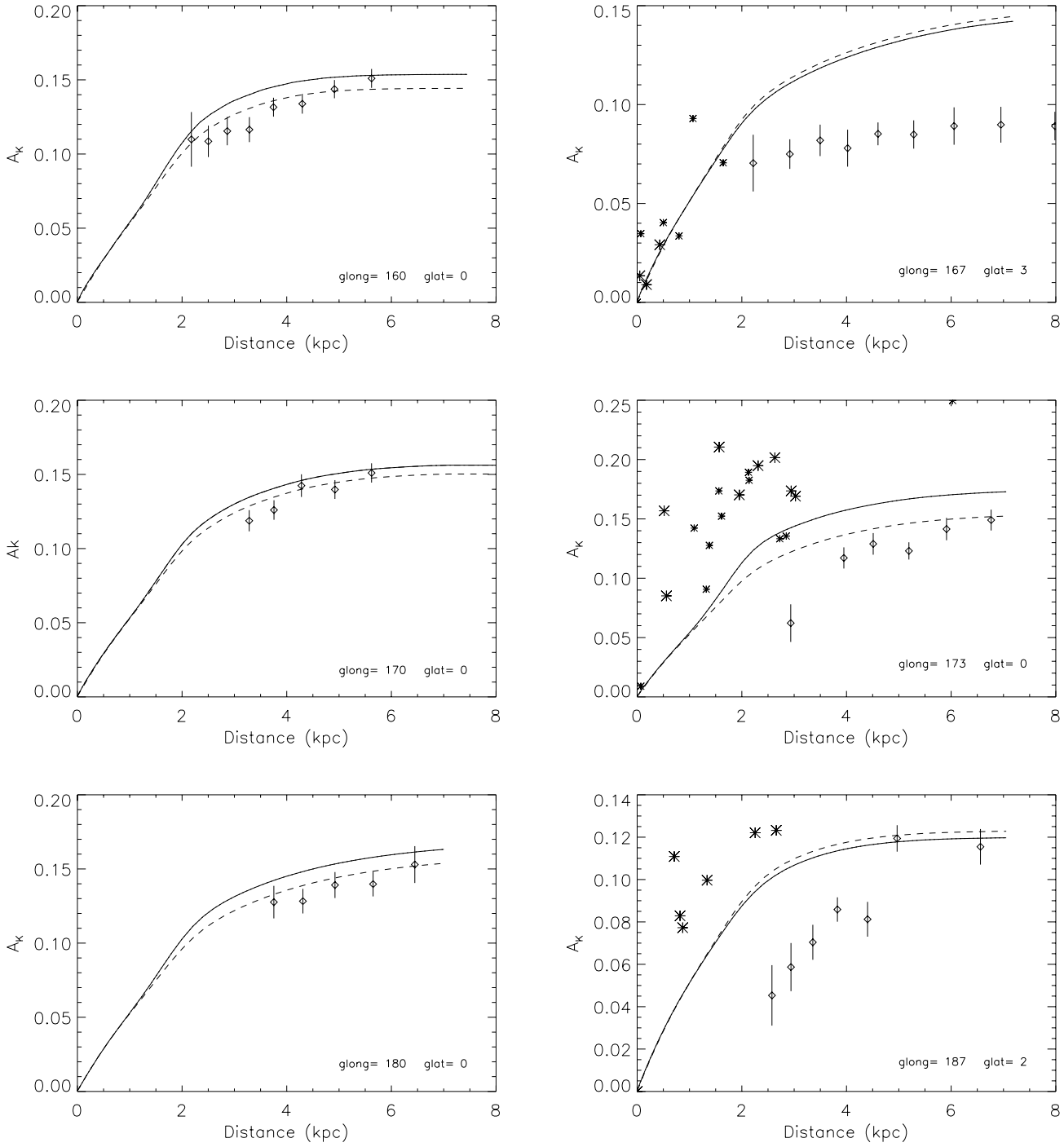

Fig. 9. *K* band extinctions along lines-of-sight in the outer disk of the Galaxy. Solid and dashed lines show the extinction according to the model presented here, with and without rescaling factors respectively. Diamonds show extinctions based on NIR CMDs of $1^\circ \times 1^\circ$ fields using 2MASS data. Asterisks show extinction measures from individual OB stars (Neckel et al. 1995), the large asterisks corresponding to stars within 0.5° of the directions indicated, small asterisks stars within 1°.

field and that at $l = 60^\circ$, the OB extinctions are higher than those given by the NIR data.

5. Summary

We have here presented a three-dimensional Galactic extinction model, based on the dust distribution model of DS01, which may be used for a variety of studies involving distant targets located in the Galactic disk or beyond. See Belokurov & Evans (2003) as an example.

Any potential user of the extinction model should be aware of a number of caveats:

1. Absorptions to points within a few hundred parsecs of the Sun will not be reliable as the spatial resolution of the dust model does not allow a detailed description of dust in the

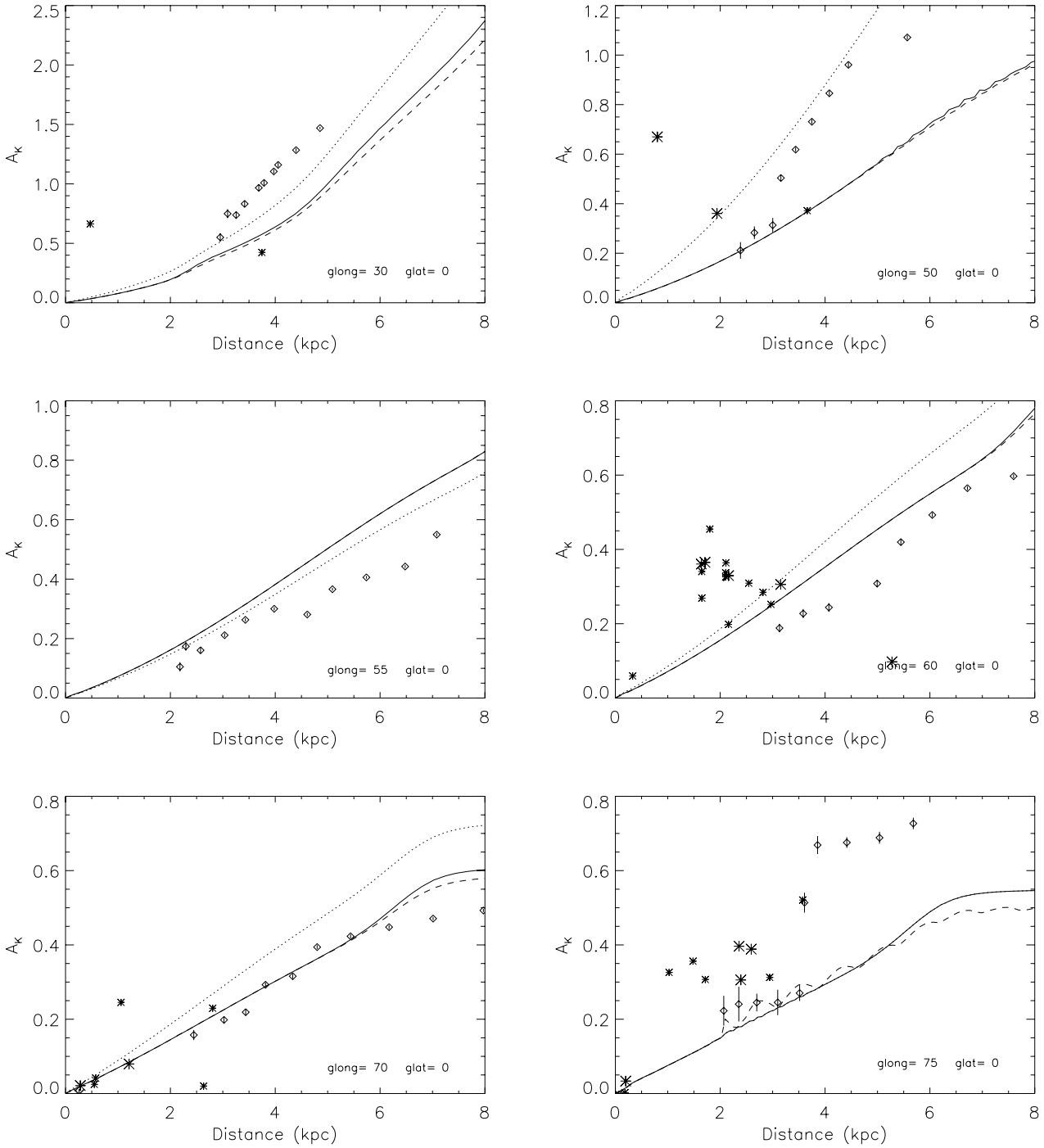

Fig. 10. *K* band extinctions along lines-of-sight in the inner disk of the Galaxy. Lines and symbols as in previous figure, with the addition of a dotted line showing the extinction of the model in the case where the disk component of the model is rescaled rather than the spiral arm component.

vicinity of the Sun. A more detailed local map of extinction is needed for nearby sources.

2. The dust model, even with rescaling, has finite angular resolution. The size of the COBE pixels are approximately $0.35^\circ \times 0.35^\circ$, with some variation over the sky. However, any field of this size (or even smaller) will contain unresolved structures in the dust distribution. Thus the run of extinction as given by the model for a given line-of-sight should be considered as a mean extinction.
3. The dust model does not include features associated with the Galactic bar nor the nuclear disk, though a central "hole" in the dust distribution is included. However, the parameters describing this hole are ad hoc as the FIR data within 20° of the Galactic center was not modeled by DS01. In addition, the adopted spiral arm geometry extend the arms too far into the center of the Galaxy, leading to arm tangents that are not evident in FIR emission in the Galactic

plane. The extinctions within 0.35 $R_\odot$ of the Galactic center may suffer significant systematic errors.

4. The density of the spiral arms are not well constrained by the COBE NIR data because the arm tangents are too distant to cause strong extinction features in the diffuse NIR radiation; lines-of-sight corresponding to arm tangents may have large systematic errors.
5. In directions where extragalactic sources contribute significantly to the FIR flux the derived rescaling factors will be erroneous. This includes the Andromeda Galaxy, M33, the LMC and SMC.
6. The rescaling factors in directions which contain anomalous dust temperatures will be in error. These include the nearby star forming regions of the Orion and rho Ophiucus complexes.

For the purpose of validating the extinction model we have also presented a method by which the extinction can be empirically estimated using NIR color-magnitude diagrams. Comparisons made for lines-of-sight in the outer Galaxy show good agreement between the model and the NIR data, showing differences less than 0.05 mag, though directions toward known OB associations have a high relative difference, in part due to anamolous dust temperatures. Toward the inner Galaxy there is less concordance, especially in directions corresponding to spiral arm tangents. Most of our comparisons with the NIR data are in the Galactic plane ($b = 0$). Interestingly the effect of the rescaling factors in the Galactic plane is not as clearly advantageous as it is at low Galactic latitudes ($|b| \approx 2{-}3^\circ$). Again, anomolous dust temperatures associated with star forming regions may be limiting the usefullness of the rescaling factors.

When reliable extinction data is available it is always preferable to rely on these rather than a model. However, even when such data is available a model may be useful to extrapolate beyond the limits of the data, as it may be able to provide extinctions at larger (or smaller) distances or at higher resolution than the data. The user is also free to compute new rescaling factors, or to rescale the entire model, when it is in clear conflict with data for a particular line-of-sight.

Some of the caveats listed above suggest possible improvements that could be made in the Galactic dust distribution model, particularly toward the Galactic center. Work is currently underway toward the development of a dust distribution model that also models the FIR emission within 20° of the Galactic center, not originally considered in the modeling of DS01. With the recent availability of high quality NIR data over the whole sky, together with methods for estimating the extinction along lines-of-sight close to the Galactic plane, it will soon be possible to improve the extinction model by providing further observational constraints. Such added constraints will be particularly helpful in deriving a more reliable estimate of the contribution to extinction from the spiral arms.

Acknowledgements. Thanks are extended to Gianpaolo Bertelli, Antonella Vallenari, Annie Robin and Francesca Figueras for testing preliminary versions of the extinction code, and to F. Figueras for contributing FORTRAN code. The first author wishes to thank Mario Lattanzi for encouragement and moral support, while financial support was provided by the Italian Ministry of Research (MIUR) under contract COFIN2001.

References

Arenou, F., Grenon, M., & Gomez, A. 1992, A&A, 258, 104
Belokurov, V. A., & Evans, N. W. 2003, MNRAS, 341, 569
Bissantz, N., & Gerhard, O. 2002, MNRAS, 330, 591
Bland-Hawthorn, J., & Maloney, P. R. 2002, in Extragalactic Gas at Low Redshift, ASP Conf. Ser., 254, 267
Blitz, L., & Spergel, D. N. 1991, ApJ, 379, 631
Chen, B., Figueras, F., Torra, J., et al. 1999, A&A, 352, 459
Davies, J. I., Trewhella, M., Jones, H., et al. 1997, MNRAS, 288, 679
Djorgovski, S., & Sosin, C. 1989, ApJ, 341, L13
Draine, B. T. 2003, ARA&A, 41
Drimmel, R. 2000, A&A, 358, L13
Drimmel, R., & Spergel, D. N. 2001, ApJ, 556, 181
Fitzpatrick, E. L. 1999, PASP, 111, 63
Freudenreich, H., Berriman, G., Dwek, E., et al. 1994, AJ, 429, L69
Georgelin, Y. M., & Georgelin, Y. P. 1976, A&A, 49, 57
Glass, I. S. 1999, Handbook of Infrared Astronomy (Cambridge University Press)
Grocholski, A. J., & Sarajedini, A. 2002, AJ, 123, 1603
Hakkila, J., Myers, J. M., Stidham, B. J., & Hartmann, D. H. 1997, AJ, 114, 2043
López-Corredoira, M., Cabrera-Lavers, A., Garzón, F., & Hammersley, P. L. 2002, A&A, 394, 883
Launhardt, R., Zylka, R., & Mezger, P. G. 2002, A&A, 384, 112
Mathis, J. S. 1990, ARA&A, 28, 37
Mendez, R. A., & van Altena, W. F. 1998, A&A, 330, 910
Neckel, T., Klare, G., & Sarcander, M. 1980, A&AS, 42, 251
Neckel, T., Klare, G., & Sarcander, M. 1995, VizieR Online Data Catalog, 2062, 0
Ortiz, R., & Lepine, J. R. D. 1993, A&A, 279, 90
Picaud, S., Cabrera-Lavers, A., & Garzón, F. 2003, A&A, 408, 141
Pietrzyński, G., Gieren, W., & Udalski, A. 2003, AJ, 125, 2494
Rieke, G. H., & Lebofsky, R. M. 1985, ApJ, 288, 618
Robin, A., & Creze, M. 1986, A&A, 157, 71
Schlegel, D. J., Finkbeiner, D. P., & Davis, M. 1998, ApJ, 500, 525+
Skrutskie, M. F., Schneider, S. E., Stiening, R., et al. 1997, in ASSL vol. 210, The Impact of Large Scale Near-IR Sky Surveys, 25
Skrutskie, M. F., Schneider, S. E., Stiening, R., et al. 2000, VizieR Online Data Catalog, 1, 2003
Spergel, D., Malhotra, S., & Blitz, L. 1996, in Spiral Galaxies in the Near-IR, ed. D. Minnitti, & H. Rix (ESO-Garching), 128
Taylor, J. H., & Cordes, J. M. 1993, ApJ, 411, 674
Wainscoat, R. J., Cohen, M., Volk, K., Walker, H. J., & Schwartz, D. E. 1992, ApJS, 83, 111
Weiland, J. L., Arendt, R. G., Berriman, G. B., et al. 1994, ApJ, 425, L81